SAND2022-5269C

Proceedings of the ASME 2022
International Mechanical Engineering Congress and Exposition
IMECE2022
October 30-November 3, 2022, Columbus, OH, USA

IMECE2022-95018

COMPARING INSTRUMENTATION SELECTION TECHNIQUES FOR VIBRATION TESTING

Moheimin Khan[1*], Justin Wilbanks[1*], Chandler Smith[1], Timothy Walsh[1], Brian Owens[1]

[1]Sandia National Laboratories
P.O. Box 5800
Albuquerque, NM, 87185

ABSTRACT

Vibration testing of complex aerospace structures requires substantial pretest planning. Ground and flight testing of structures can be costly to execute in terms of time and money, so it is pertinent that tests are properly set up to capture mode shapes or dynamics of interest. One of the most important planning tasks is the placement of sensors to acquire measurements for control and characterization of the results. Without properly placed sensors, dynamics of interest could be missed or improperly characterized in subsequent modeling efforts. Both outcomes can be deleterious to the data collected in addition to the quality of vibration environment reconstruction in the laboratory. In this paper, we will examine two techniques that can leverage available output from finite element modeling to intelligently choose locations to place accelerometers for a vibration test to capture the structural dynamics throughout a specified frequency range with a set data acquisition channel budget. These two techniques are effective independence (EI) and optimal experimental design (OED). Both methods will be applied to an aerospace structure consisting of multiple subassemblies. A finite element model of the structure will be leveraged to supply the input data for the approaches as well as examine the quality of the resulting instrumentation sets. Metrics, such as the auto modal assurance criterion (Auto-MAC), will be used to quantify the quality of the instrumentation set chosen. The effect of chosen sets on system equivalent reduction and expansion process (SEREP) will also be detailed. In addition to comparing the resulting instrumentation sets, the application of the two approaches will be compared in terms of the inputs required, the information obtained from their application, and the aggregate computation time requirements. The utilization of EI to "warm-start" the OED approach will also be explored to determine if there is any benefit in computation time without comprising the final instrumentation set selection. Impact of the input data used to inform the selection strategies will be examined by using data from decoupled subassemblies of the structure as well as the complete structure. The results will provide additional understanding of the impact of the coupling of the substructures on the selection strategies. Sensitivity of both approaches to instrumentation type, uniaxial or triaxial, will be compared based on the chosen accelerometer locations. These studies will inform the best application for each selection method, in terms of the inputs required from finite element models, overall workflows, and instrumentation set information provided.

Keywords: Vibration Testing, Test Planning, Optimization

NOMENCLATURE

EI	Effective Independence
DOF	Degree of Freedom
FRF	Frequency Response Function
MAC	Modal Assurance Criterion
OED	Optimal Experimental Design
RMS	Root Mean Square
SEREP	System Equivalent Reduction Expansion Process

1. INTRODUCTION

Properly instrumenting an assembly for vibration testing is paramount to the resulting data quality and post-test analyses. Various methods exist to choose a possible instrumentation set for a vibration test. A popular approach introduced by Kammer is effective independence, what we will denote as EI in this paper [1]. This method can be computationally inexpensive and aims to minimize the condition number of the Fisher information matrix for the modes of interest. This method has been studied by several groups in various applications. Meo and Zumpano, leveraged EI for health monitoring in civil engineering structures and compared it to other approaches comparisons [2], Papadopoulos and Garcia compared EI to other placement strategies for dynamic testing of a Euler-Bernoulli beam and structural frame [3], Friswell and Castro-Triguero demonstrated the clustering issue that can occur with EI [4], and Kim *et al.* extended the method by developing a stochastic version of the

*Equal Contribution.

approach [5]. The EI method is straightforward to implement, and a workflow can be developed that leverages the tools available for an analyst or test engineer.

Various other methods have been proposed and demonstrated throughout the aerospace and civil engineering communities. Suryanarayana *et al.* demonstrated a data-based method leveraging the Hilbert Schmidt Independence Criterion and a grey-box building model to develop the approach [6]. Clark *et al.* demonstrated the use of a method based on a QR decomposition method to minimize the reconstruction error in problems using a linear map for reconstruction with the measured values at the sensors for various problem types [7]. Finally, Beale *et al.* demonstrated the use of optimal experimental design to place sensors for a multiple-input/multiple-output (MIMO) vibration test [8]. This method was selected due to its combability with existing workflows as an alternative approach for designing an instrumentation set in this paper using Sierra SD to generate the required input data and MATLAB to complete further analyses.

Section 2 defines the structural dynamic model of the aerospace structure and the analyses completed to support the application of the EI and OED instrumentation selection approaches. Section 3 introduces the two approaches and explores their application to the chosen structure. Section 4 provides various comparisons between the sets chosen with EI and OED. Finally, Section 5 provides a conclusions and possible future work.

2. DEFINITION OF STRUCTURE FOR ANALYSIS

The structure of interest for this work is an assembled configuration of previous research articles studied at Sandia National Laboratories. The assembled structure is termed the Wedding Cake and Removable Component Assembly (WRCA) and consists of the Wedding Cake (WC) structure from [9] and the Removable Component (RC) subassembly from [10]. The two subassemblies are attached to a shell structure, which contains a base support for the WC and a plate for the RC. An image of the assembly is shown in FIGURE 1. The WRCA was developed as an exemplar for investigating instrumentation design approaches for assembled aerospace structures with dynamics of interest in the bandwidth of 20 to 2000 Hz.

2.1. Finite Element Model of Dynamic System

The structure was modeled using in-house software packages at Sandia National Laboratories, including CUBIT for the meshing [11] and the Sierra Structural Dynamics (Sierra/SD) linear finite element code for the dynamic analysis [12]. Modal and modal random vibration analysis was performed, and the results were used for subsequent instrumentation selection studies.

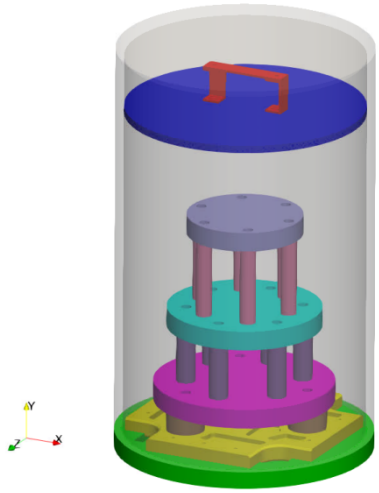

FIGURE 1: IMAGE OF STRUCTURE FOR ANALYSIS.

2.2. Modal Solution

Sierra/SD was used to perform modal analyses of the system and its subassemblies. Modes were computed up to 2000 Hz, with a free-free boundary condition for the instrumentation design with EI and fixed-base for the subsequent random vibration loading and definition of the FRF arrays for the OED implementation. Free-free boundary condition was used for EI since it is a typical starting point for analysis and model calibration and allows for direct comparison to experimental data that is available during test design. For the assembled free-free case, 60 modes were computed in the bandwidth. A selection of elastic modes is shown in FIGURE 2 and the natural frequencies associated with all computed modes are provided in Table A1.

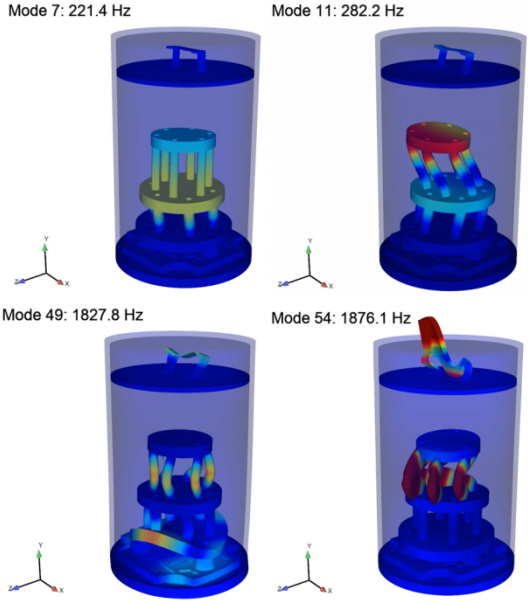

FIGURE 2: SELECT ASSEMBLY MODES.

In addition, modes of each subassembly (WC, RC, and Shell) were computed up to 2 kHz. FIGURE 3 shows a selection of elastic modes for each subassembly. Modes from both the

assembly and subassembly configurations were utilized to compare the different instrumentation selection strategies. If it doesn't affect performance, considering the subassemblies separately can provide more flexibility in a test plan as well as provide individual instrumentation sets that can be used for testing articles separately.

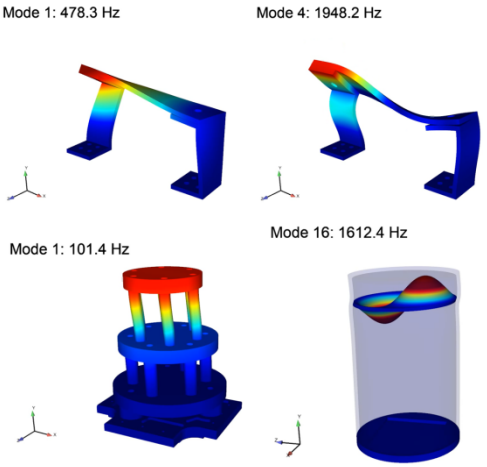

FIGURE 3: SELECT SUBASSEMBLY MODES.

2.3. Random Vibration Solution

Random vibration was selected as the loading condition of interest for this work since it is a common environment for aerospace structures. A 0.1 g^2/Hz flat random, Gaussian white noise from 20 to 1000 Hz was used as the input, shown in FIGURE 4.This bandwidth was selected to limit the effects of modal truncation using the structure modes out to 2 kHz.

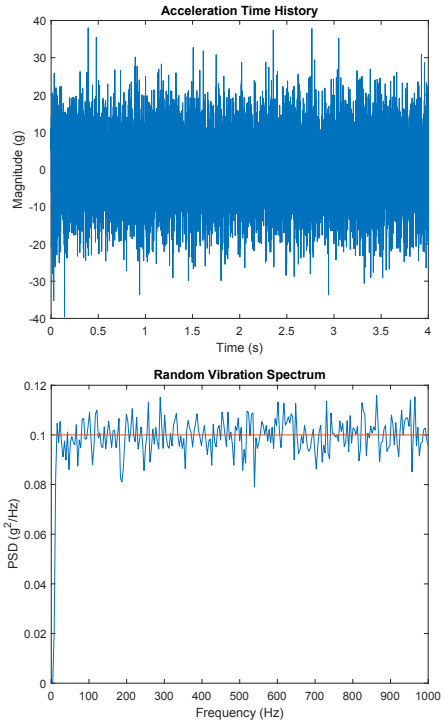

FIGURE 4: RANDOM VIBRATION LOADING.

The dynamic analysis was conducted with Sierra/SD, using a seismic mass and rigid elements for base excitation. A transient simulation was performed with a force applied to the seismic mass via rigid elements. The resulting acceleration time history of the random vibration is applied to all points on the base of the structure. Loading was applied in the transverse X-axis direction, illustrated in FIGURE 5. This modeling approach simulates single axis fixed-base vibration testing typically conducted on a shaker table.

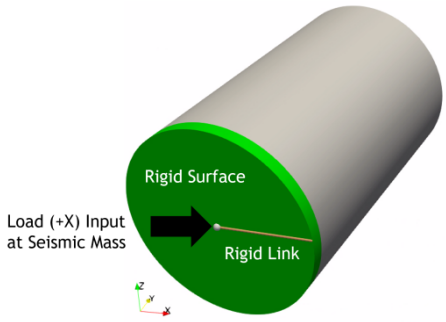

FIGURE 5: LOAD APPLICATION.

The results from the random vibration analysis were subsequently used for expansion studies with System Equivalent Reduction Expansion Process (SEREP) and to evaluate the effectiveness of the various instrumentation sets. Once an instrumentation set is defined and test data collected, SEREP allows engineers to expand from the instrumented locations to other points within a test article leveraging analysis data. A good instrumentation set allows for an effective expansion that can provide a complete picture of the response of a test article with limited measurement points.

3. INSTRUMENTATION SELECTION STRATEGIES

Two major techniques were used for the instrumentation selection: Effective Independence (EI) and Optimal Experimental Design (OED). The instrumentation selection workflow for each approach is outlined in FIGURE 6.

First a finite element mesh of the structure of interest is generated using CUBIT. Candidate surfaces are selected based on available locations for accelerometers. Next, candidate nodes on each surface are generated using a subset of the nodes. These are typically determined based on an evenly spaced cartesian or cylindrical grid dependent on the surface and part geometry. Local coordinate systems are then created for each candidate point. This process has been semi-automated using MATLAB scripts and an example of the resulting outputs is shown in FIGURE 6. The outputs include a mesh file that contains the coordinate locations chosen as well as a channel table that can be read into either MATLAB or Microsoft Excel.

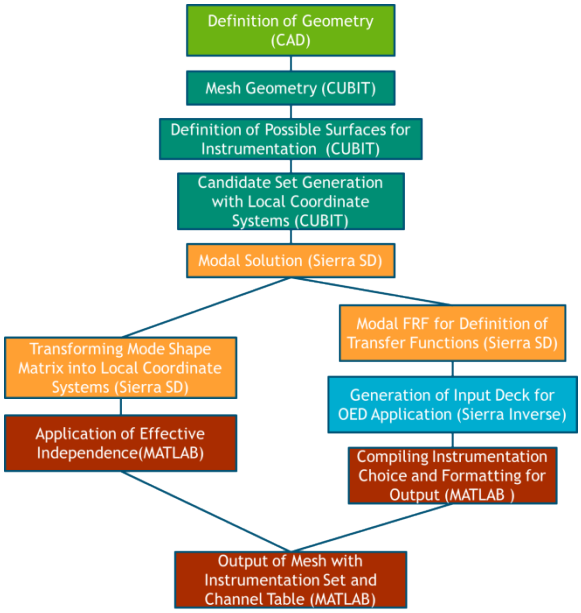

FIGURE 6: WORKFLOW FOR EI AND OED WITH SOFTWARE CHOICES HIGHLIGHTED IN EACH STEP.

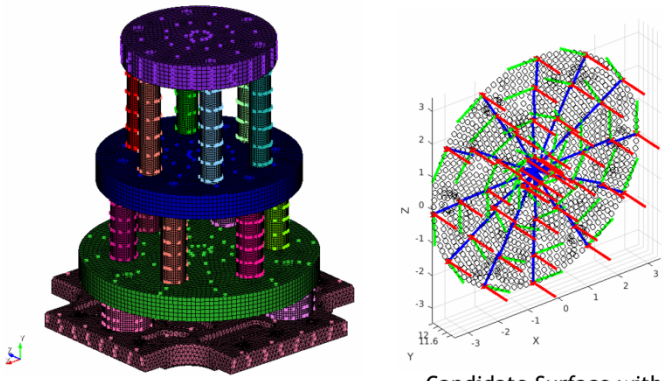

WC with Candidate Nodes

Candidate Surface with Coordinate Systems

FIGURE 7: INSTRUMENTATION DESIGN EXAMPLE FOR WC.

After the candidate set has been determined, a modal solution is performed with Sierra/SD, with mode shapes output at each candidate node location. The subsequent steps vary based on the desired instrumentation selection technique. As stated before, FIGURE 6 provides an overview of the workflow leveraged for both the EI and OED approaches. Compared to EI, OED requires an additional analysis with Sierra/SD that outputs the transfer functions from the input location of the test to the candidate gauge locations. Section 3.1 and 3.2 detail the two selection strategies used within MATLAB with the intermediary outputs from our FEA software for structural dynamics problem at Sandia National Laboratories, Sierra/SD. The optimization problem for OED is also completed with the Sierra environment.

The computation time associated with EI corresponds to a modal analysis of the test article of interest in Sierra/SD as well as the EI implementation in MATLAB with output data of Sierra/SD. In comparison, OED requires the modal analysis in addition to a modal FRF solution to obtain the required transfer functions. Finally, the OED approach is implemented in the Sierra environment. Sierra runs can be run in parallel to help improve speed. The EI implementation in MATLAB is typically fast enough to not require parallelization, taking under 3 minutes for the assembly level set. The computation times are dependent on how many processors that are used. The modal run is approximately 1/3 the computation time of the modal FRF runs for the six degrees of freedom, where the modal run was approximately 5 minutes. In addition, OED can be anywhere form 5-100 times the computation time required for the modal run. These run times are associated with different machines with multiple processors, so direct time comparisons are difficult. OED doesn't require significantly more setup time than EI; however, it does require additional computational resources.

3.1. Effective Independence Introduction

Effective independence is a commonly used method to determine placement of accelerometers for vibration testing. Kammer introduced effective independence in identifying instrumentation locations for testing of aerospace structures [1]. Effective independence is a sub-optimal approach since it is implemented iteratively to determine the least impactful sensor location during each iteration [1, 4]. Effective independence is built upon the foundation of the Fisher information matrix (Q):

$$Q = \Phi^{\mathrm{T}}\Phi \tag{1}$$

where Φ denotes the mode shape matrix and Φ^T the transpose of the mode shape matrix.

EI is implemented in MATLAB [1, 4] iteratively by calculating the orthogonal projection matrix:

$$E = \Phi^{\mathrm{T}}\mathrm{Q}^{-1}\Phi \tag{2}$$

where Q^{-1} denotes the inverse of the Fisher information matrix. In this process, the minimum diagonal term of E are identified and the associated instrumentation location and degree of freedom is removed from the candidate set. This process can be defined such that uniaxial accelerometers, triaxial accelerometers, or a combination of both (hybrid) can be used. This is implemented by either grouping degrees of freedom or considering them individually. The iterations continue until the channel required channel budget is met.

Once an instrumentation set is selected with EI, the auto Modal Assurance Criterion (MAC) and condition number of the reduced mode shape matrix is calculated to determine the quality of the resulting set. The auto-MAC between modes i and j is given as:

$$\mathrm{MAC_{ij}} = \frac{\left[\Phi_i\Phi_j\right]^2}{\left[\Phi_i^{\mathrm{T}}\Phi_j\right]\left[\Phi_j^{\mathrm{T}}\Phi_i\right]} \tag{3}$$

where Φ_i is the modal vector for mode i and Φ_j is the modal vector for mode j. The Auto-MAC measures the independence of the modes of the system of interest and has a value from 0 to 1, where 1 denotes a significant similarity between mode shapes [13].

3.2. Optimal Experimental Design Introduction

The other method leveraged in this paper to choose an instrumentation set is OED. OED poses the instrumentation design task as a convex optimization problem. Beale *et al.* demonstrated the instrumentation problem in the context of OED [8]. The instrumentation set design problem can be posed as a least-squares problem:

$$\bar{s}(\theta) = min(\frac{1}{2}\|T(\theta)s - y_M\|_2^2) \tag{4}$$

where $T(\theta) = Q_O(\theta)H$ and y_M is a set of measurements from experiment or finite element model at n points in either the complex or real domain. $Q_O(\theta)$ is an observation operating with a parameter set θ signifying the possible degrees of freedom at the various instrumentation locations. H denotes the transformation from the unknown parameters, s, to the measurement locations, y_M. The dimension of H is $n \times p$ in the complex or real domain.

Equation (4) has the following closed-form solution:

$$\bar{s}(\theta) = (T(\theta)^* T(\theta))^{-1} T^*(\theta) y_M \tag{5}$$

where $()^*$ denotes the complex transpose. The minimization process seeks to minimize an uncertainty-based metric, which can also be viewed as maximizing the acquired information [8].

For I-optimality criterion, the optimal degrees of freedom solve the following convex optimization problem:

$$\begin{aligned} \bar{\theta} &= \min\,(\frac{1}{n}\sum_{i=1}^{i=n} H_i^* C(\theta) H_i) \\ s.t. \quad & \sum_i \theta_i = 1, \;\; 0 \le \theta_i \le 1 \end{aligned} \tag{6}$$

where $C(\theta)$ denotes the covariance of the estimated parameters and is defined by:

$$C(\theta) = \mathbb{E}[\bar{s}(\theta)\,\bar{s}^*(\theta)] = \sigma^2 (T(\theta)^* T(\theta))^{-1} \tag{7}$$

where σ is the variance [8]. H_i is the i^{th} column of the H, which is the frequency response function (FRF) array for the WRCA assembly with a fixed base. This array is acquired, as outlined in FIGURE 6, using Sierra SD. The optimal instrumentation, or parameter set, implies that the model's average prediction variance is minimized, denoted as $var(\hat{y}_i)$ [8]. Since OED is convex, the optimal solution is the global minimizer.

The output of the optimization problem is an instrumentation set alongside a probability measure of the chosen sensor location. Each probability is between 0 and 1. When the optimization constraints are met and the solution converges, the sum of all probabilities will be equal 1. These probabilities allow one to see the importance of each chosen instrumentation location, which provides additional utility beyond EI [8]. However, OED provides slightly less control over the number of locations chosen as well as how many locations are chosen for each subassembly. This is an important consideration, since it is often desirable to be able to perform component and subassembly level design which can work at the assembly level. It is difficult to enforce total sensor budget constraints for OED since these constraints are inherently non-convex. Current research is focusing on how to implement these types of constraints. Section 3.4 provides a brief overview of the instrumentation set chosen through OED. Section 4 provides comparisons between the OED set and the sets chosen with EI.

3.3. Application of Effective Independence

The Effective Independence method was used to generate instrumentation sets for both the assembly and subassembly configurations. A predefined instrumentation budget of 80 channels or degrees of freedom (DOF) was established for the WRCA to adequately cover the 60 modes up to 2 kHz. For the subassemblies, 8, 40, and 32 DOF were split between the RC, WC, and Shell, respectively. The budget used is higher than would be considered for a physical test. Often, our budget constraints can be limited to available space or DAQ channels. Ongoing work focuses on methods to reduce the channel budget while maintaining the performance of the chosen set. Instrumentation studies with EI were performed for cases with triaxial, uniaxial, and a hybrid of triaxial and uniaxial sensors. FIGURE 8 shows the resulting downselected instrumentation sets for the hybrid approach and FIGURE 9 through FIGURE 11 display the individual subassembly sets.

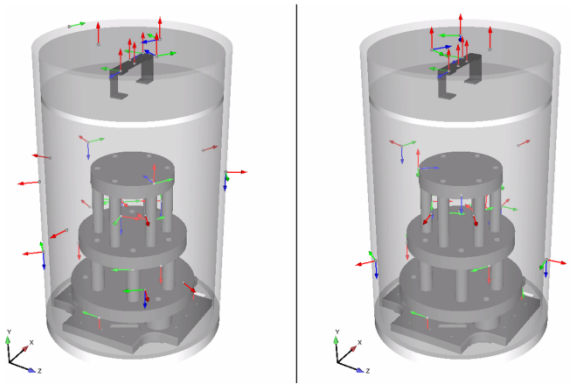

FIGURE 8: EI HYBRID WRCA SETS.

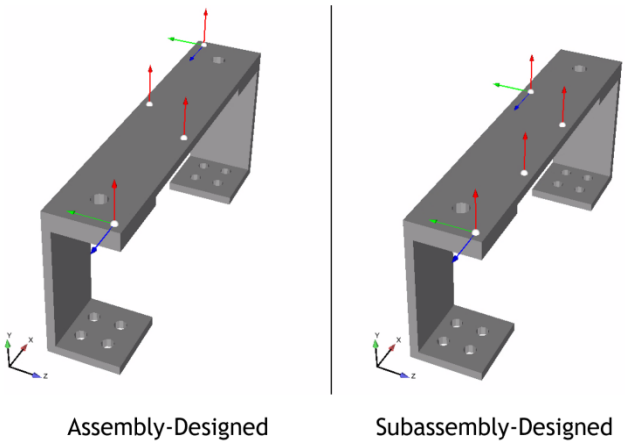

FIGURE 9: EI HYBRID RC SETS.

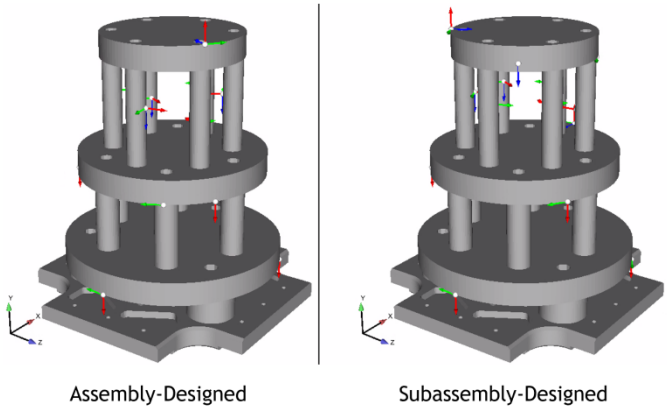

FIGURE 10: EI HYBRID WC SETS.

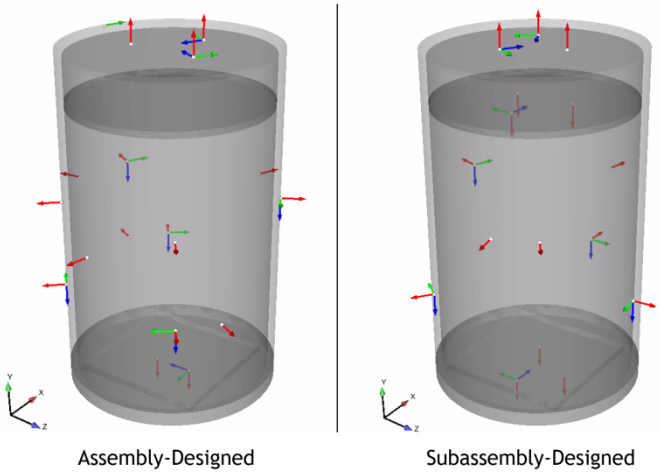

FIGURE 11: EI HYBRID SHELL SETS.

The instrumentation sets for each case appear visually similar and both assemblies have the same number of DOF, although not equally split between subassemblies. As mentioned previously, one popular method used to evaluate the quality of an instrumentation set is by computing an Auto-MAC, given in Eq. (3), which computes the similarity of modes. The auto-MAC for the WRCA assembly-designed and subassembly-designed sets is provided in FIGURE 12.

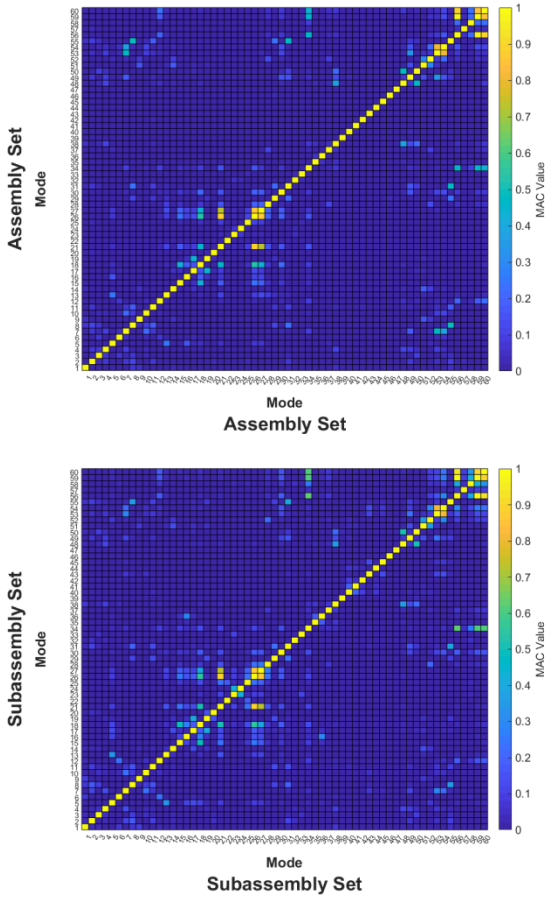

FIGURE 12: WRCA AUTO-MAC.

The vast majority of the 60 WRCA modes are independent and well-captured by each set, indicated by the low off-diagonals in the Auto-MAC. There are a select few modes that with a high off-diagonal MAC (even more so for the subassembly-designed set) but overall, both methods appear to provide similar instrumentation sets using EI. Subsequent sections will use expansion and other metrics to further compare the sets in detail.

3.4. Application of Optimal Experimental Design

FIGURE 13 shows the instrumentation set chosen with OED. The same candidate set used with EI was leveraged in the OED process. The FRF array was formed by taking the input location as the seismic mass shown in FIGURE 5. All FRFs were generated from 100 Hz to 2000 Hz at a frequency step of 1 Hz in Sierra SD. The OED process can be expensive computationally; therefore, a coarser frequency set of frequency lines can be used for the FRF array, such as 3 or 6 points per octave. Additionally, the subassemblies could be considered separately by dividing up the FRF array and candidate sets for each subassembly and then conducting the optimization for the subassemblies individually. A complete instrumentation set could then be generated by

combining the final solutions. This can also provide additional flexibility in the final chosen set.

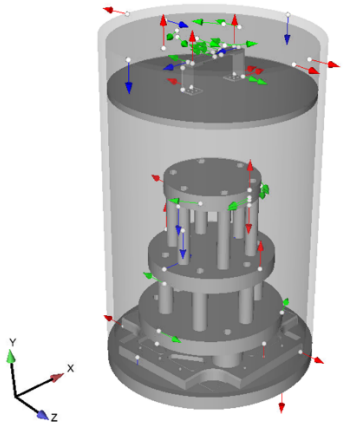

FIGURE 13: OED WRCA SET.

The Auto-MAC for the first 22 modes of the WRCA is given in FIGURE 14 for the OED instrumentation set. The set shown in FIGURE 13 and FIGURE 14 were generated with a relatively coarse frequency line step with 3 points per octave from 100 Hz to 2000 Hz. The set was generated by considering each subassembly separately with the FRF array defined using the complete WRCA assembly. Observing FIGURE 14, the Auto-MAC is comparable to EI; however, the Auto-MAC for the OED set deteriorates for modes 23 through 29 as shown in FIGURE 15. Even though the Auto-MAC measure is slightly worse for the OED set, the expansion metrics shown in Section 4 are better for the OED set compared to the EI sets. Modes 23 through 29 may not contribute significantly in aggregate to the system response and FRFs used in the OED process, so placements that can capture these modes may be overlooked in lieu of areas that contribute more to the overall system response.

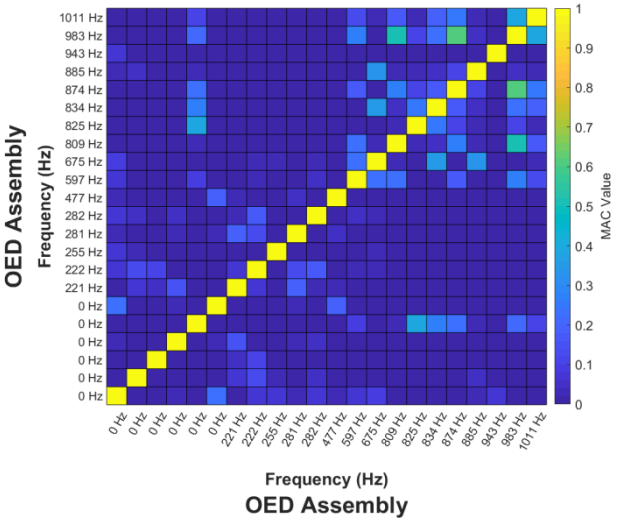

FIGURE 14: OED WRCA AUTO-MAC.

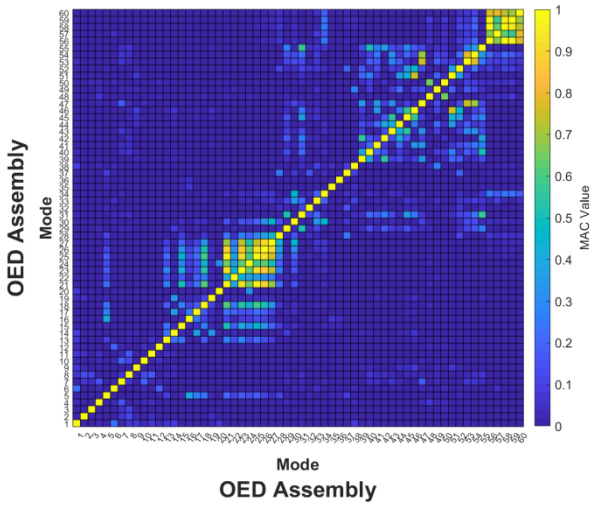

FIGURE 15: OED WRCA AUTO-MAC TO 2 KHZ.

OED was also applied to a fixed-based version of the RC mesh to generate a FRF array for just the RC component. FIGURE 16 compares the OED set generated for the RC with the assembly and subassembly data. The sets are comparable with the subassembly set requiring less instrumentation locations for convergence of the optimization problem.

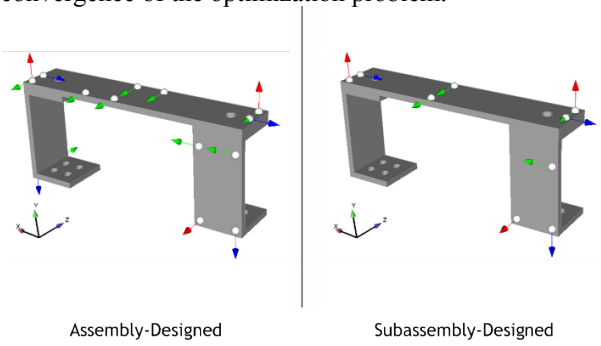

FIGURE 16: COMPARISON OF OED SET GENERATED WITH ASSEMBLY OR SUBASSEMBLY DATA.

The Auto-MAC for the assembly with the new RC locations is provided in FIGURE 17. It is very similar to the Auto-MAC of the assembly set provided in FIGURE 14. Mode 18 consists of significant RC motion and the Auto-MAC is improved in the RC subassembly set.

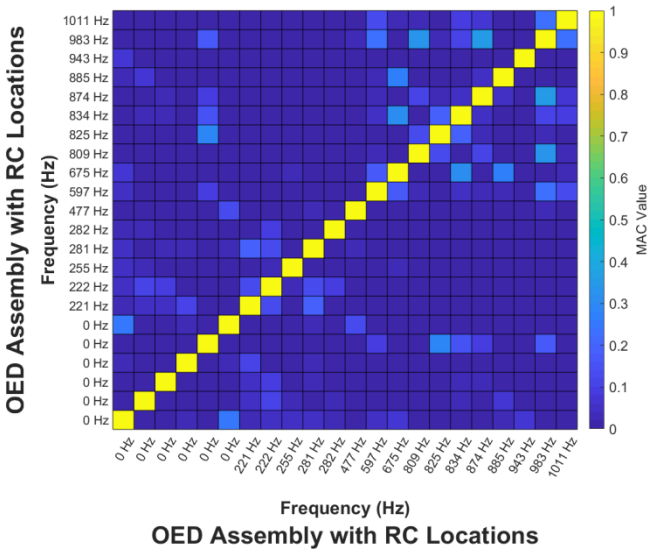

FIGURE 17: OED WRCA AUTO-MAC WITH RC LOCATIONS DEFINED USING RC SUBASSEMBLY ANALYSIS.

4. COMPARISON AND ANALYSIS OF INSTRUMENTATION SETS

To quantitatively compare the resulting instrumentation sets from the EI and OED methods, the following metrics were utilized:

1. Auto-MAC
2. Condition Number
3. Mean Absolute Peak Error
4. Root Mean Square Error

As stated before, the Auto-MAC provides both a visual and numeric measure of the independence of each mode in the set relative to the others. A lower off-diagonal Auto-MAC means that the modes can be distinguished from each other, for example while extracting modal parameters with experimental data. Mathematically, the condition number evaluates the sensitivity of an output to changes in the input. In our case, it also gives a numerical measure of mode independence, where a low value (often below 100) is desired for processing using expansion or other techniques such as sub-structuring [1].

Th error metrics were selected to give a quantitative measure of the expansion results. The mean absolute peak error measures the accuracy of the peak response and the root mean square (RMS) error also identifies low or high overall bias in the expanded vibration response.

4.1. Auto Modal Assurance Criterion and Other Direct Metrics

First, the quality of the various EI instrumentation sets will be compared using the Auto-MAC and condition number. TABLE 1 lists the max off-diagonal Auto-MAC and condition numbers of the full candidate set and subassembly sets. Considering the subassemblies individually increases the condition number over an order of magnitude, from 53.4 to 829.1. This change is likely due to the fixed base approximation of the RC used in the process. In the full assembly, there are higher-order modes near 2 kHz which contain significant motion of the RC mounting plate. One example is mode 59, shown in FIGURE 18. This relative motion would not be adequately captured by fixing the bottom of the RC legs, as was done in the subassembly instrumentation design. This could negatively impact the response recorded for the RC, and is one example of possible detriment that could arise from considering subassemblies separately. This impact will depend on how much boundary conditions of the assembly don't align with the simple subassembly boundary conditions that could be imposed.

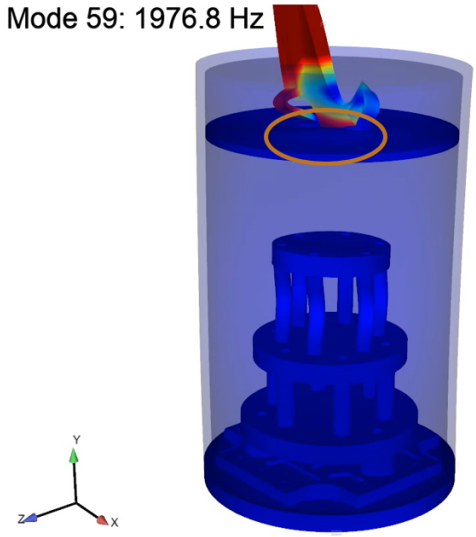

FIGURE 18: WRCA MODE WITH RC LEG RELATIVE MOTION HIGHLIGHTED.

The effect of these local RC leg modes can be further demonstrated by removing them from the set and re-evaluating the condition number. TABLE 1 shows that removing these modes from the subassembly set can result in Auto-MAC and condition numbers close to the assembly set. The relationship between condition number and number of modes kept was studied for the EI sets and plots are provided in FIGURE 19 and FIGURE 20. As more modes are added, the condition number increases as expected. However, the increase for the subassembly set is drastic after mode 51. Again, this is due to the poor approximation of RC legs being fixed since modes 50 to 60 have significant motion of the plate the RC is mounted on.

The sensitivity of each DOF in the set can be evaluated as well and this relationship is plotted for each case in FIGURE 20. Evaluating the removal of any individual DOF emphasizes the relative stability and importance of the DOF in the instrumentation set. Sets with uniaxial accelerometers appear to be more sensitive to a given DOF while the assembly case with only triaxial accelerometers resulted in locations with high insensitivity to loss. This sensitivity is important to consider during experiments and would inform possible backups if a

sensor was lost during testing, for example. The triaxial sensor case also provided the lowest condition number as shown in TABLE 3, although results were comparable to the other methods.

TABLE 1: AUTO-MAC AND CONDITION NUMBER FOR EI INSTRUMENTATION SETS.

Case	Max Off-Diagonal Auto-MAC	Condition Number
Full Candidate Set	0.81	9.18
Assembly Set	0.97	53.4
Subassembly Set	0.98	829.1
Subassembly Set without mode 59	0.93	587.7
Subassembly Set without modes 53,54,56,59	0.88	76.7

Additionally, EI results can be used to warm-start the OED process or to provide additional information about the importance of each chosen sensor. OED was able to be implemented without warm-starting and it provided a better final set using the full candidate. Using the EI subset limits the possible selection of gauges for OED. This can create an issue with the overall instrumentation choice since channel budget constraints cannot be enforced directly. Therefore, it is possible for OED to converge with a relatively small set of gauges that can impact overall performance in terms of the metrics considered. A possible alternative to make warm starting more effective is to use EI to downselect to a relatively large possible instrumentation set and use OED to further reduce the set. Adding in an effective channel budget constraint to OED, either minimum or maximum channel definition, would further increase the applicability of warm starting the OED process with EI or other methods.

Using the EI output to define a smaller candidate set for OED to determine the importance of the chosen candidate sets in the uniaxial EI case. The top five gauges based DOF probability is contained in TABLE 2. DOF indices 14,62, and 71 are all pertinent for the uniaxial EI case and 2 and 30 are elevated in the EI assembly case. Therefore, OED also can be used to help determine the importance of gauges once selected and could be supplemented with information from EI.

TABLE 2: TOP FIVE OED GAUGE SELECTIONS BASED ON PROBABILITY VALUES.

DOF Index	Max Off-Diagonal Auto-MAC
2	1
14	0.86
62	0.80
71	0.67
30	0.65

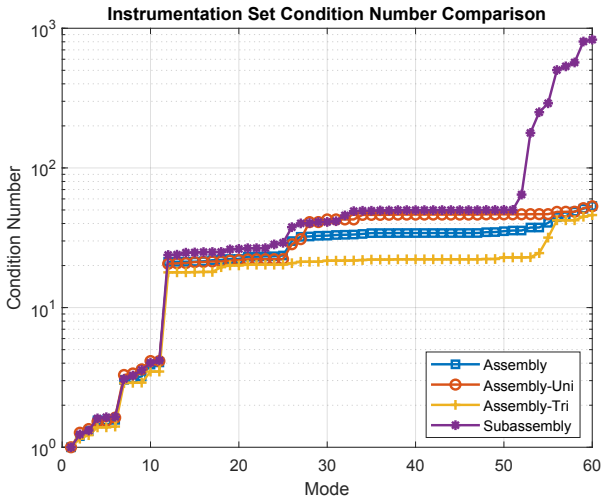

FIGURE 19: EI CONDITION NUMBER VERSUS MODE.

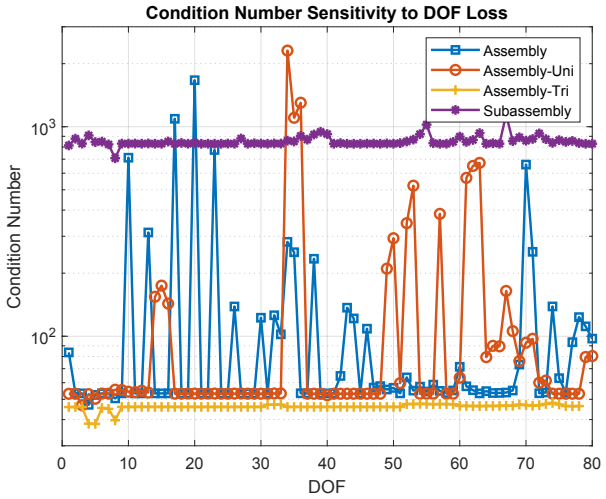

FIGURE 20: EI CONDITION NUMBER VERSUS SENSOR DOF LOST.

TABLE 3: AUTO-MAC AND CONDITION NUMBER FOR EI SETS BASED ON SENSOR TYPE.

Case	Max Off-Diagonal Auto-MAC	Condition Number
Hybrid Method	0.97	53.4
Uniaxial Only	0.97	53.2
Triaxial Only	0.96	46.0

TABLE 4 provides the max off-diagonal Auto-MAC and condition number for the instrumentation set chosen with OED. The condition number for the OED sets, with the RC locations defined with assembly and subassembly data, is higher than both

EI sets for 22 and 60 modes. Off-diagonal Auto-MAC values are comparable between the EI and OED sets for 60 modes.

TABLE 4: AUTO-MAC AND CONDITION NUMBER FOR OED INSTRUMENTATION SETS.

Case	Max Off-Diagonal Auto-MAC	Condition Number
OED Assembly (22 Modes)	0.61	153.24
OED Assembly [RC] (22 Modes)	0.36	140.78
OED Assembly (60 Modes)	0.98	1931.70
OED Assembly [RC] (60 Modes)	0.99	1680.30

4.2. Impact of Selection Techniques Applied on Modal Expansions

SEREP was used to expand the random vibration response from a point in each instrumentation set to a new point on the RC. A comparison of the expanded response was performed with the different instrumentation selection strategies for both EI and OED. The point, highlighted in FIGURE 21, is part of the original candidate set and was chosen as an example where response is desired on a component or subassembly, in a location that was not instrumented.

Simulated test data was generated by adding Gaussian white noise to the responses obtained from the Sierra/SD simulations. A signal to noise ratio of 20 dB was chosen, which is a minimum value recommended by [14] for dynamic measurements. In addition, all data was filtered using a band pass from 20 to 1000 Hz.

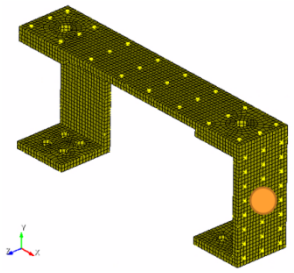

FIGURE 21: EXPANSION POINT ON RC.

The expansion results for a 50-millisecond portion of the random vibration loading are plotted in FIGURE 21 and the error metrics are summarized in TABLE 5. In addition, the power spectral density responses are provided in FIGURE 23. Immediately, both the assembly and subassembly responses at the RC point appear very close to the simulation-generated test response, with some noticeable differences in the power spectrum above 800 Hz. For the time history, the error magnitude is low, about 1g, and most of the discrepancies are at the peaks. Still, the error is lower for the assembly set- about 30% for the mean absolute peak error. This result is consistent with the higher quality observed earlier in the condition number and Auto-MAC, but the changes are not as drastic for the expanded response.

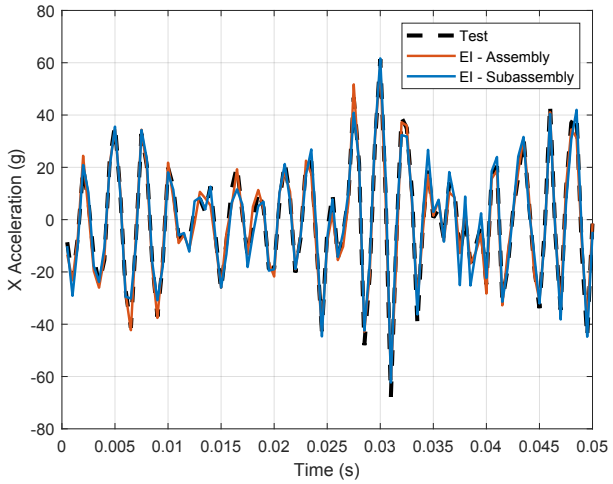

FIGURE 22: EXPANSION COMPARISON FOR EI INSTRUMENTATION SETS.

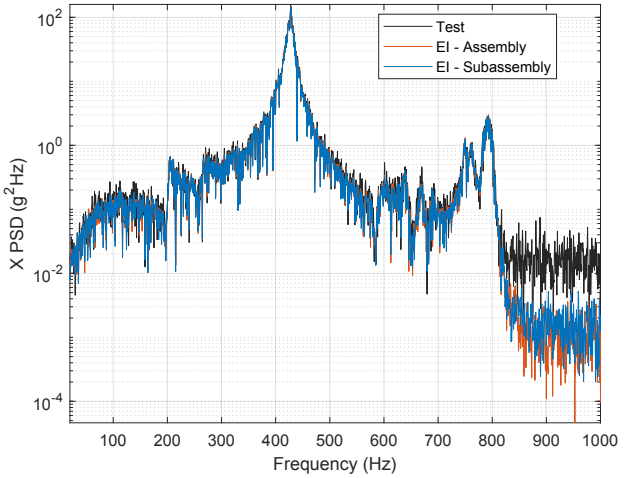

FIGURE 23: EXPANSION PSD COMPARISON FOR EI INSTRUMENTATION SETS.

TABLE 5: EXPANSION COMPARISON METRICS FOR EI INSTRUMENTATION SET.

Metric	Assembly Set	Subassembly Set
Mean Absolute Peak Error (g)	0.788	1.130
RMS Error (g)	-0.962	-0.963

The RC expansion for the OED sets with the RC instrumentation locations defined with assembly and subassembly data is provided in FIGURE 24. The corresponding

error metrics are provided in TABLE 6. Both the mean absolute peak and RMS errors are lower for the OED sets, using the assembly and subassembly RC locations, compared to the EI instrumentation choices. The subassembly OED case is denoted with [RC] in TABLE 6. Figure 25 provides the power spectral density responses for the OED instrumentation sets compared to the EI assembly set. The OED also performs well for frequencies up to 800 Hz for the simulation-generated data representing a set of test data. At 800 Hz, the PSD deviates slightly form what the simulation-test data is, which could result from the deviations observed in the Auto-MAC for both the OED and EI sets.

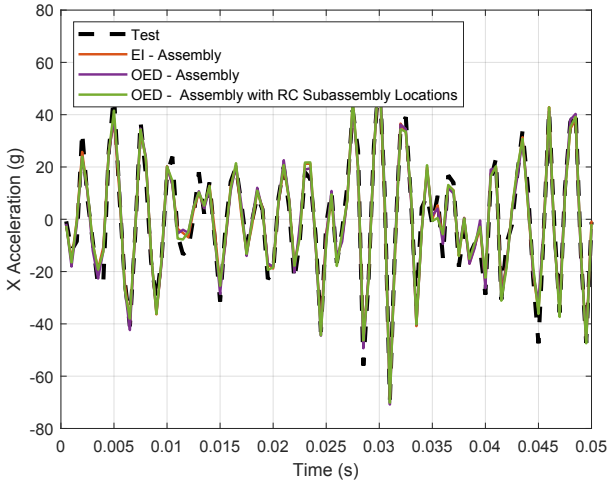

FIGURE 24 EXPANSION COMPARISON FOR OED INSTRUMENTATION SETS.

TABLE 6: EXPANSION COMPARISON METRICS FOR OED INSTRUMENTATION SETS.

Metric	OED	OED [RC]
Mean Absolute Peak Error (g)	0.003	0.354
RMS Error (g)	0.005	-0.426

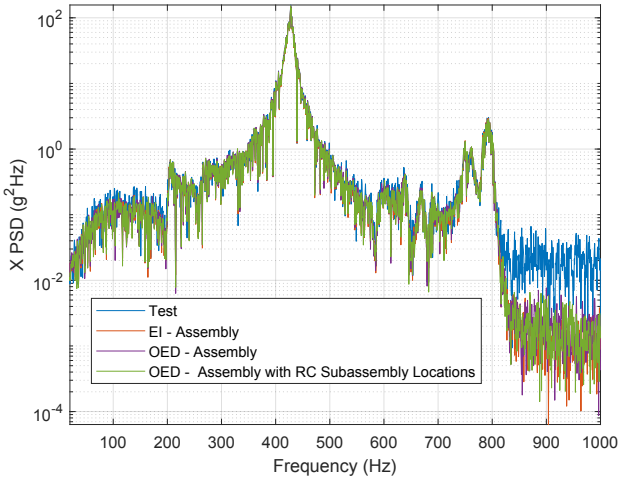

FIGURE 25 EXPANSION PSD COMPARISON FOR OED INSTRUMENTATION SETS.

Compared to the Auto-MAC and condition number, the expansion results were much more consistent for the instrumentation sets. Both quantitatively and qualitatively, each method provided an expanded response that was close to the simulated test response. This is a stark contrast to the condition number, which varied nearly two orders of magnitude depending on the set. One major factor is that the responses used in expansion were filtered to 1 kHz and the instrumentation sets perform much better in this bandwidth, as mentioned in section 3.4. A different expansion point may not perform as well, but these results indicate that all the instrumentation sets adequately capture the dynamics of the RC.

5. CONCLUSION

Both OED and EI offer an effective method for selecting an instrumentation set for a given vibration test. EI is a straightforward, computationally inexpensive approach that provides effective instrumentation sets for vibration testing in terms of modal analysis and SEREP expansion of the results. It also offers the flexibility to use uniaxial gauges, triaxial gauges, or a combination of both. OED is also an effective approach that is slightly more expensive computationally. EI only requires a modal analysis whereas OED requires a FRF array to be developed form the input location for a test to the prospective measurement points. Additionally, the OED optimization implementation can be more expensive than the iterative optimization process used for EI. OED is less sensitive to the impact of local modes in the definition of the instrumentation set. OED provides a natural ranking of importance of each chosen DOF, which can be extremely helpful. EI doesn't automatically provide this but can be leveraged in such a way to provide arbitrary numbers of redundant, or additional, gauges to fit a specific channel budget. OED provides an effective alternative that can be improved with some small changes. Future work could consider implementing channel budget constraints that would provide needed flexibility to reduce required OED runs as well as more exploration of using EI to warm-start the OED selection approach. Also, improving the efficiency of OED relative to EI would help increase its applicability.

6. APPENDIX

TABLE A1: NATURAL FREQUENCIES FOR WRCA MODE SHAPES.

Mode Number	Frequency [Hz]	Mode Number	Frequency [Hz]
7	221.404	35	1625.64
8	221.96	36	1626.09
9	255.244	37	1640.83
10	280.597	38	1655
11	282.241	39	1764.49
12	477.357	40	1767.47
13	596.614	41	1775.52
14	674.978	42	1781.09
15	809.248	43	1781.38

16	824.767	44	1783.63
17	833.891	45	1783.69
18	874.089	46	1791.35
19	885.444	47	1792.03
20	942.987	48	1801.55
21	982.563	49	1827.79
22	1011.34	50	1837.16
23	1011.8	51	1852.93
24	1022.15	52	1857.9
25	1022.4	53	1874.15
26	1112.02	54	1876.09
27	1206.06	55	1894.03
28	1328.69	56	1958.37
29	1344.64	57	1963.51
30	1439.56	58	1963.85
31	1490.66	59	1976.84
32	1508.59	60	1982.53
33	1509.49	61	2143.12
34	1549.44		

ACKNOWLEDGEMENTS

Sandia National Laboratories is a multimission laboratory managed and operated by National Technology & Engineering Solutions of Sandia, LLC, a wholly owned subsidiary of Honeywell International Inc., for the U.S. Department of Energy's National Nuclear Security Administration under contract DE-NA0003525.

REFERENCES

[1] Kammer, D. C., 1991, "Sensor placement for on-orbit modal identification and correlation of large space structures," *J Guid Control Dyn*, 14(2), pp. 251-259.

[2] Meo, M., and Zumpano, G., 2005, "On the optimal sensor placement techniques for a bridge structure," *Eng. Struct.*, 27(10), 1488-1497.

[3] Papadopoulos, M., and Garcia, E., 1998, "Sensor placement methodologies for dynamic testing," *AIAA J*., 36(2), pp. 256-263.

[4] Friswell, M. I., and Castro-Triguero, R., 2015, "Clustering of sensor locations using the effective independence method," *AIAA J*, *53*(5), pp. 1388-1391.

[5] Kim, T., Youn, B. D., and Oh, H., 2018, "Development of a stochastic effective independence (SEFI) method for optimal sensor placement under uncertainty," *Mech. Syst. Signal Process.*, 111, pp. 615-627.

[6] Suryanarayana, G., Arroyo, J., Helsen, L., and Lago, J., 2021, "A data driven method for optimal sensor placement in multi-zone buildings," *Energy Build.*, *243*, pp. 110956.

[7] Clark, E., Askham, T., Brunton, S. L., and Kutz, J. N., 2018, "Greedy sensor placement with cost constraints," *IEEE Sens. J.*, 19(7), pp. 2642-2656.

[8] Beale, C., Schultz, R., Smith, C., and Walsh, T., 2022, "Degree of Freedom Selection Approaches for MIMO Vibration Test Design," Proceedings of IMAC XL, Orlando, FL, February 7-15, 2022.

[9] Beale, D., Owens, B., and Schultz, R., 2020, "Analysis of full-field response from a multi-shaker test," Proceedings of IMAC XXXVIII, Houston, TX, February 10-13, 2020.

[10] Rohe, D. P., Smith, S., Brake, M. R., DeClerck, J., Blanco, M. A., Schoenherr, T. F., and Skousen, T. J, 2019, "Testing summary for the box assembly with removable component structure," ," Proceedings of IMAC XXXVII, Orlando, FL, January 28-31, 2019.

[11] CUBIT Development Team, "CUBIT Geometry and Mesh Generation Toolkit 15.8 User Documentation," 2021, Sandia National Laboratories Technical Report: SAND2021 -5152 W.

[12] Crane, N. K., Day, D. M., Hardesty, S., Lindsay, P., and Stevens, B. L 2020, "Sierra/SD - User's Manual - 4.56", Sandia National Laboratories Technical Report SAND2020 3828.

[13] Allemang, R. J., 1982, "A correlation coefficient for modal vector analysis," Proceedings of the International Modal Analysis Conference, Orlando, FL, November 8-10, 1982, pp. 110-116.

[14] Csurcsia,P. Z.,Peeters, B., Schoukens, J., and De Troyer, T. 2020, "Simplified Analysis for Multiple Input Systems: A Toolbox Study Illustrated on F-16 Measurements," Vibration, 3(2), pp. 70-84